

IMAGE-BASED 3D TORSO BODY MODELING

3D Female Body Modeling for Breast Surgery Simulation

Youngjun Kim, Kunwoo Lee

Human-Centered CAD Lab., Seoul National University, ShilimDong, KwanakGu, Seoul, Korea

Wontae Kim

K&I Technology, 1586-6, SeochoDong, SeochoGu, Seoul, Korea

Keywords: Human body, image-based 3D modeling, breast surgery.

Abstract: This paper proposes an image-based 3D modeling algorithm for a 3D torso of the human body. This approach provides an easy and practical way of modeling so that doctors can obtain the subject's 3D data without additional equipment such as a 3D scanner or MRI. To achieve this goal, a 3D template model with feature points is prepared, and then a 3D model of the subject is reconstructed from orthogonal photographs by deforming the 3D template model. An appropriate number of feature points and their positions are derived. Procrustes Analysis and Radial Basis Functions (RBFs) are applied for the deformation. After the deformations, images are mapped onto the mesh for realistic visualization.

1 INTRODUCTION

Three dimensional human body modeling is one of the most popular topics in the computer animation and reverse-engineering fields. There are various ways to get 3D human data, such as 3D scanning, direct modeling, example-based modeling, etc. Among them, image-based 3D human modeling is one of the most attractive methods due to its simplicity and practicality. However, although many approaches have been applied to the face, few trials have been done especially for the breast or torso area. Image-based upper body modeling is more difficult than face or head modeling because the upper body has fewer dominant feature points.

The goal of this project is to develop virtual simulation software for breast plastic surgery. For breast surgeries, including breast augmentation and other cosmetic purposes, virtual simulation may play an important role in discussions between doctors and patients. It also helps surgeons decide the best way to operate. Many 2D simulation programs have already been developed, but they lack realism, and most are unnatural. For 3D breast simulation, Balaniuk et al. implemented a 3D breast surgery simulation using REM (Balaniuk, et al., 2006). They are getting good results, but they use a 3D scanner to get the subject's body data and they simulate only

the breast. Our approach overcomes those weaknesses. In this paper we propose a simple way to reconstruct a female torso from photos. This is the first stage of the virtual simulation for breast surgery. We need only several photos of the subject, and we can get a realistic 3D model of the upper body. Based on the ideas of image-based head modeling, we present efficient algorithms to generate a 3D torso model from several images of a subject. For this purpose, a template model with feature points and segments is prepared. We deform the template model to get the subject's 3D data, using orthogonal images of that person.

The remainder of the paper is organized as follows. Section 2 describes the template model to be deformed, and Section 3 explains the algorithms of deformation to get the subject's 3D model. The results of our work are described in Section 4, and future work is discussed in Section 5.

2 TEMPLATE MODEL PREPARATION

2.1 3D Template Model

A generic model, or template model, is commonly used for image-based body modeling. We call the 3D model a template model in this paper to avoid confusion. The template model must have a typical and representative shape. The mesh data should be neat and clean. Because no template model data can represent all body types, several types of template models should be prepared. However, acquiring and standardizing many scanned data of naked bodies are not easy. For these reasons, we made template models using modelling tools, rather than by scanning an actual human body. We used MAYA 7.0 to make the 3D template model. Figure 1 shows the template data.

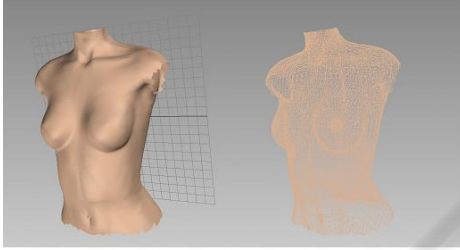


Figure 1: A refined 3D template model: mesh display mode (left) and wire-frame display mode (right).

2.2 Feature Point Definition

Feature points are necessary and important prerequisites to get a realistic result in image-based modeling. We referred to Lee's definition (H. Lee, K. Hong and E. Kim, 2004), and excluded some points and defined some additional points for our purpose. The number of feature points is 10 for the left and right breasts, respectively. The two side-view images are scaled according to the height of the breast, from P0 to P4, in the front-view image. For the abdominal part, 18 feature points (six points each for the left, right and central waist curves, respectively) are defined. These points are automatically positioned by skin detection as described in Section 3.2. Additional points such as navel, armpit, shoulder, etc. are also defined. Table 1 and Figure 2 show the definitions of the feature points.

Table 1: The definition of the feature points.

Pt	Definition
P0	Upper breast point (UBP), same y-coord. as LAP on C_{bf} & C_{bs}
P1	Mid-point of P0 & P2 on C_{bs}
P2	Bust point (BP) on C_{bf} & C_{bs}
P3	Mid-point of P2 & P4 on C_{bs}
P4	Bottom breast point (BBP) on C_{bf} & C_{bs}
P5	Mid-point of P0 & P6 on C_{bf}
P6	Outermost point on C_{bf}
P7	Mid-point of P6 & P4 on C_{bf}
P8	Mid-point of P4 & P9 on C_{bf}
P9	Inner breast point (IBP),
FNP	Front neck point
SP	Shoulder point, same y-coord. as FNP
CSP	Center of shoulder point on C_{bf} , mid-point of FNP & SP in x-dir.
OBP	Outer breast point on C_{bf} , mid-point of P0 & P4 in y-dir.
WP1	Same y-coord. as P4, on C_w or C_c
WP2 ~ WP5	Equally dividing points between WP1 and WP6 in y-dir. on C_w or C_c
WP6	Same y-coord. as P4, on C_w or C_c
FCP	Front center point, Mid-point of LBP9 & RBP9
NP	Navel point, the same point as WP6 on C_c

I_f : front-view image, I_s : side-view image
 C_{bf} : breast curve in I_f C_{bs} : breast curve in I_s
 C_w : waist curve in I_f C_c : belly curve in I_s

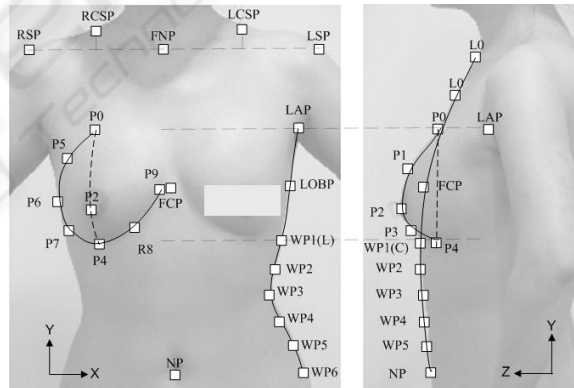


Figure 2: Definitions of the feature points (R: right, L: left, C: centre).

3 TEMPLATE MODEL DEFORMATION

3.1 Image Capture

In our image-based 3D torso body modeling, we use a front-view and two side-view photographs of the subject. We need both the left-view and right-view images in order to reconstruct breasts that are not symmetrical. A back-view photograph is optionally added if needed for texture mapping. We define the

feature points from these orthogonal images. The image for the texture mapping is also obtained from them. Many postures of the subject were tested considering the texture mapping and repeatability. A white or blue background is recommended because we detect the body curves by skin detection.

An image-capturing device is designed to get the photos conveniently even though our software allows any kind of digital images of subjects. Our image-capturing device, which is connected to a PC with a USB cable, consists of a digital camera and a distance-checking sensor. The image captured by the digital camera is sent directly to our software. Olympus SDK v3.3 is applied to implement remote-capturing (<http://www.olympus.com/>). An ultrasonic sensor checks the distance from the object and gives the distance information to our software. We can roughly calculate the actual size of the subject using calibration information according to the distance. The images of several discrete positions of a calibration panel are taken beforehand. Our system's distance range is 1-2m. Tsai's calibration method is applied to derive the relations between the image coordinates and the world coordinates at each position. Figure 3 shows our image-capturing device and the calibration panel.

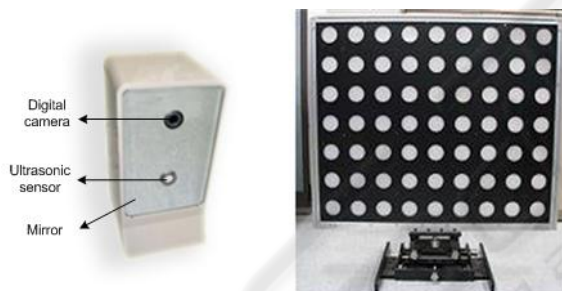


Figure 3: Photos of the image-capturing device (left) and the calibration panel (right).

3.2 3D Feature Points' Calculation from Images

After taking pictures or loading the images of the subject, we assign the feature points. All of the points or each point can be scaled and translated easily with our GUI. Some points are constrained by the definition in Table 1, and many of them are automatically positioned. For example, RSP and LSP have the same y-coordinates as FNP. Their coordinates in the front-view image are set at the outmost positions of the body at the FNP's y-level.

In Section 2.2, the feature points P0, P2 and P4 in the front-view image are assumed to lie on the same plane in the 3D coordinate system. These points are also defined in the side-view. Therefore,

x- and y-coordinates are assigned in the front-view image and z- and y-coordinates are decided in the left-view image. Internally, the side-view images are scaled and normalized according to the front-view. With these relationships, the coordinates of all the feature points are derived. Their x-coordinates are obtained from the front image, and the z-coordinates are computed from the side image. The y-coordinates are common values in the front and side images. The amount of proper deformation of the template model is obtained by the process of matching the corresponding feature points in the template to those in the images. Sections 3.3 and 3.4 describe the algorithms in detail.

WP1~WP6 are detected automatically using skin detection. We used YCbCr colour space. We need to handle only Cb and Cr values because we are interested in the illumination intensity invariant part of the colour for the skin detection. Eq. (1) below shows our skin detection criteria:

$$\{p(x, y) | Cb_{\min} < Cb < Cb_{\max} \& Cr_{\min} < Cr < Cr_{\max}\} \quad (1)$$

where

$$Cb_{\min} = 77, \quad Cb_{\max} = 132$$

$$Cr_{\min} = 133, \quad Cr_{\max} = 171$$

In the skin detection process, we have many small holes in the interior of the body. These holes are obstacles to finding the body's curves, so we fill the holes if they are smaller than a threshold size proportional to the image size. Figure 4 shows the skin detection result and the feature points.

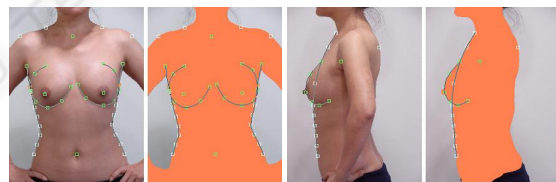


Figure 4: Skin detection result and feature points on 2D front-view (left) and left-view (right) images. Some of the points are positioned manually and the others are set automatically.

3.3 Global Deformation

In the global deformation step, we compute the affine transformation matrix to match the template model as closely as possible to the feature points calculated from the images. The affine transformation includes translation, rotation and scaling. To minimize the sum of the squared error between the calculated feature points and the corresponding feature points of the transformed model, we use Procrustes Analysis (J.C. Gower and G.B. Dijksterhuis, 2004). This method is computationally simple and stable. This global deformation is an auxiliary step because it gives

good initial conditions for local deformation. Normalization of the data is also done in this step.

$$\min E(S, R, T) = \sum (P_C - P_T)^2 \quad (2)$$

where

P_C : Feature points calculated from images
 P_T : Feature points of template model

$$P_T = \begin{bmatrix} x_T \\ y_T \\ z_T \end{bmatrix} = S \cdot R \begin{bmatrix} x_{T0} \\ y_{T0} \\ z_{T0} \end{bmatrix} + T$$

S : scale factor
 R : rotation matrix
 T : translation vector

The procedures of the global deformation are as follows:

- Compute the mean of both P_T and P_C .
- Center each set at its origin.
(i.e., $P_{C0} = P_C - \text{mean}(P_C)$)
- Compute the norm of each set $\|P_{C0}\|^2$ and $\|P_{T0}\|^2$.
- Normalize each set to equal the unit norm.
(i.e., $P_{C0} = P_C / \|P_{C0}\|^2$)
- Let $A = P_{C0}^T P_{T0}$.
- Compute the Singular Value Decomposition (SVD) of A that results in the matrices L, D and M.
(i.e., $LDM = SVD(A)$)
- Compute the rotation matrix $R = ML^T$.
- Compute the scaling factor.
$$S = \sum \text{diagonal}(D) \times \frac{\|P_C\|^2}{\|P_T\|^2}$$
- Compute the translating vector.
$$T = \text{mean}(P_{C0}) - (S) \text{mean}(P_{T0})(R)$$
- Transform P_T to P_C using $P_T' = S \cdot P_T \cdot R + T$.
- Finally, transform the entire 3D template model's vertices using S, R and T .

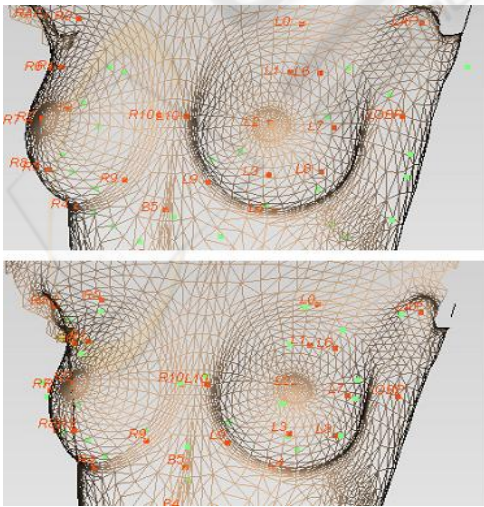


Figure 5: Before and after global deformation; red points are P_T and green points are P_C .

3.4 Local Deformation

After global rigid deformation aligns the template model to P_C , local deformation refines and generates a more realistic model. For this process, an interpolation function is estimated, and the rest of the points are mapped using this function. Among the interpolation methods, Radial Basis Function (RBF) is a powerful technique for interpolating in a multidimensional space (Ruprecht and Müller, 1993., Carr, et al., 2001., Park, et al., 2005., etc). The basis function, $R(d)$, depends only on the distance from the feature points, which are thus called radials. RBF constructs the interpolant as a linear combination of basis functions and then determines the coefficients of the basis functions. The concept of RBF is that each vertex is influenced by all the feature points, but the near feature points are more influential on that vertex.

$$f(p) = \sum_{i=1}^N w(i) R(\|p - p(i)\|) \quad (3)$$

where

$f(P)$: transformed vertex through local deform
 $w(i)$: coefficients of the basis functions
 $p(i)$: model's feature points
 p : each vertex of generic model (input point)

The most common radial basis functions, $R(d)$, are as follows:

$R(d) = d$	(linear)
$R(d) = d^3$	(cubic)
$R(d) = d \log(d)$	(thin plate spline)
$R(d) = (d^2 + c^2)^{u/2}$	(multiquadric)
$R(d) = e^{-dc^2}$	(Gaussian)

We tested those radial basis functions and selected the most appropriate one for our model:

$$R(d) = e^{-d/50^2} \quad (4)$$

To find the coefficients of the basis functions, $w(i)$, we have Eq. (4) letting $f(P_T)$ and P_C be equal.

$$p_{xC}^j = f_x(p_{xT}^j) = \sum_{i=1}^N w_x(i) R(\|p_{xT}^j - p(i)\|) \quad (5)$$

where $j = 1, 2, \dots, N$

p_{xC}^j : the x-coordinate of the j^{th} calculated feature point

p_{xT}^j : the x-coordinate of the j^{th} template model feature point after global deformation

Because we have N pairs of p_{xC}^j and p_{xT}^j , we can solve Eq. (5) and get the basis functions' coefficients.

$$\begin{bmatrix} w_x(1) \\ w_x(2) \\ \vdots \\ w_x(N) \end{bmatrix} = H^{-1} \begin{bmatrix} p^1_{Cx} \\ p^2_{Cx} \\ \vdots \\ p^N_{Cx} \end{bmatrix} \quad (6)$$

where

H is a matrix which consist of radial basis function values.

With the same steps above, we deform in the y- and z-directions also. We apply RBF for all vertices of template mesh data and finally get the morphed data according to the subject.

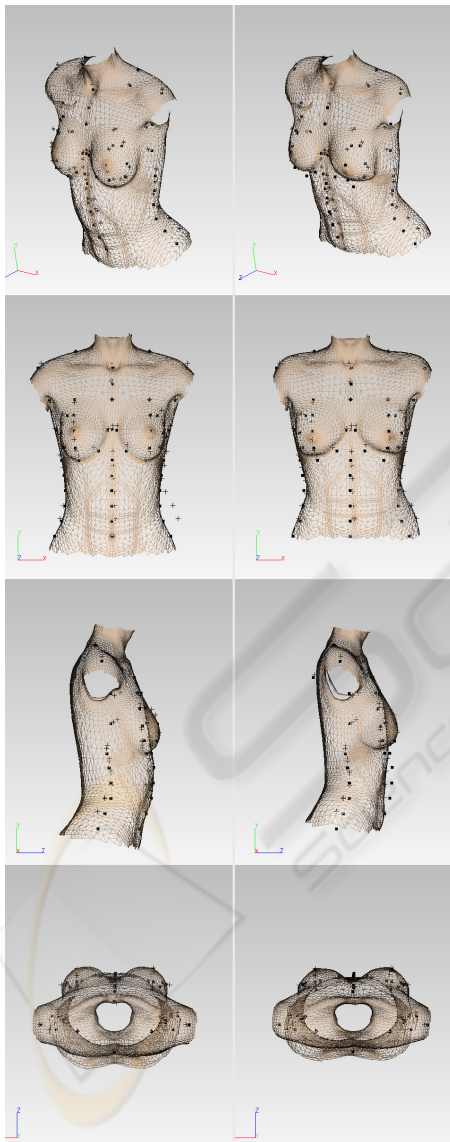


Figure 6: Before and after local deformation from several views (dot mark: P_r , cross mark: P_c).

3.5 Texture Mapping

For realism, the texture image is mapped onto the deformed mesh data. The subject's front-view and side-view images are used for texture mapping. Because we have already assigned feature points on the images, the texture coordinates of each vertex are easily calculated. The main issue in texture mapping is how to blend the three or four orthogonal images. We checked the normal direction of facets to decide the blending ratio. Here, let us assume that we use front-, left- and right-view images for the texture mapping. The front-view and side-view images are orthogonal, so the blending ratio is calculated by the normal vector's Z component. At this time, the left image should be used only for the left part ($x > 0$), and vice versa for the right part. When we add the back-view image, the blending algorithm is similar, too. Eq. (7) explains our texture image blending method in detail.

$$\begin{aligned} &\text{if } x > 0 \text{ (i.e. left part),} \\ &\quad \text{if } \bar{n}_x > 0, \\ &\quad\quad \alpha_f = \bar{n}_z, \alpha_l = 1 - \bar{n}_z \\ &\quad \text{else} \\ &\quad\quad \alpha_f = 1, \alpha_l = 0 \\ &\text{if } x < 0 \text{ (i.e. right part),} \\ &\quad \text{if } \bar{n}_x < 0, \\ &\quad\quad \alpha_f = \bar{n}_z, \alpha_r = 1 - \bar{n}_z \\ &\quad \text{else} \\ &\quad\quad \alpha_f = 1, \alpha_r = 0 \end{aligned} \quad (7)$$

where

\bar{n}_x, \bar{n}_z : X and Z component of the normal vector, respectively

The normal vectors are normalized.

$\alpha_f, \alpha_l, \alpha_r$: the blending ratio of front, left and right images for texture mapping, respectively.

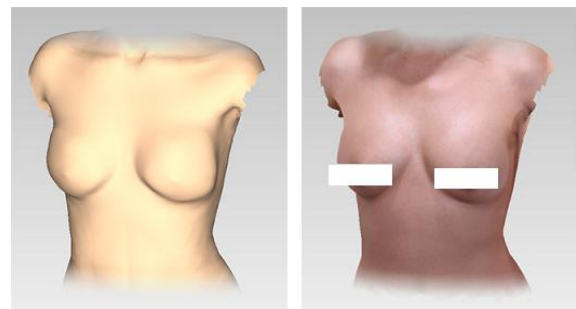


Figure 7: The resulting 3D data from a subject's photographs: the geometrical shape (left) and the textured model (right).

4 RESULTS

This paper proposes an image-based 3D torso modeling method. A template data is prepared, and the efficient number and positions of the feature

points are verified. We have developed and applied several geometric deforming algorithms and a texture mapping method to get the subject's 3D data from images. We also have designed an image-capturing device to approximate the actual size. We can measure dimensions or volumes of a subject's data if we reconstruct the 3D data in actual size. The remote-capturing function enables the operator to take digital images handily. In Figure 8 shows the result of our work compared to front-view photos. As the figure indicates, both the 3D geometry and texture information of each subject are reconstructed well for the purpose of visualization.

We analyzed the results by comparing them to the subjects' actual 3D scan data. Table 2 shows those results. RapidForm2002 was used to analysis the distance errors (<http://www.rapidform.com>). The errors are rather big due to the limitations of the image-based approach. The different postures of the subjects increased the errors. However, our result is realistic enough to meet our original goal, which is virtual simulation of breast surgery. Moreover, our method requires only three orthogonal images and needs no expensive hardware. It takes only about a minute to get the results, starting from capturing a subject's photos. We are convinced that the proposed method can be applied to animation or other computer graphics with no problem.

To increase the proposed approach's reliability, some plastic surgeons and implant retail dealers have participated and shared their know-how in the development process.

5 FUTURE WORK

The final goal of this project is to develop a 3D breast surgery simulation system; thus a new algorithm is needed to deform a subject's current 3D model to see the virtually changed appearance after the surgery. One possible method for this simulation would be to use the displacement vectors of the feature points between before and after the operation. Our image-based 3D modeling algorithm will be applied to get subject's 3D data before and after plastic surgery for the existing cases. The relationship between before and after the operation would be derived by synthesizing or averaging the transform vectors. Then the deformed feature points would be obtained from the relationship, and finally the simulated 3D data would be obtained by applying RBF interpolation. Because 3D data are available only if the transformed feature points are given, this scenario is plausible and reasonable. For this purpose, we are gathering orthogonal images of patients before and after plastic surgery. For realistic

simulations, it is also necessary to construct a database of body shapes according to implant types and sizes. It would be also possible to make other cosmetic surgery simulation software for the face and other parts of the body by extending the scenario described above.

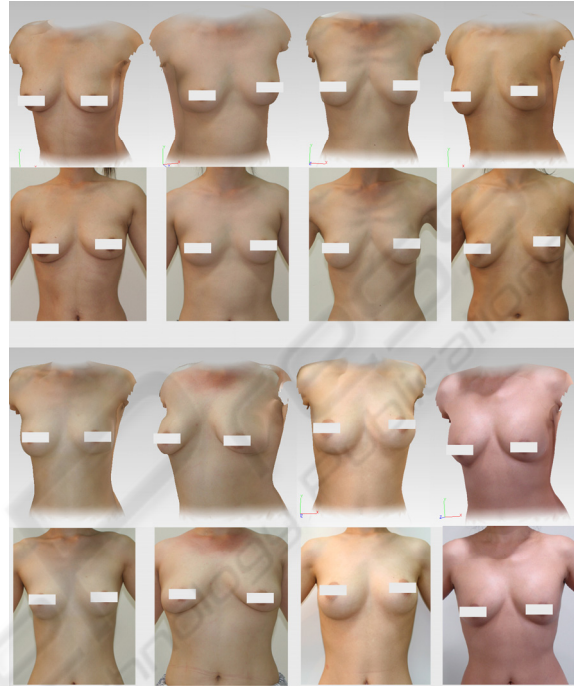


Figure 8: Examples of eight female subjects. Upper rows are snapshots of the reconstructed 3D data, and lower rows show real frontal photos of each subject.

Table 2: Distance errors between the reconstructed data and the scanned data of the subjects. (unit: [mm], SD: standard deviation).

No.	Min.	Max.	Mean	SD
1	-14.2	15.3	0.05	5.41
2	-25.0	17.8	0.41	5.45
3	-14.6	20.6	0.57	5.72
4	-24.2	27.5	-0.87	9.23
5	-14.1	13.8	0.28	6.40
6	-19.0	25.5	1.57	7.87
7	-18.3	19.7	0.67	5.91
8	-15.7	13.8	-0.72	5.89

ACKNOWLEDGEMENTS

We would like to thank K&I Technology and Woorhi Trading for their technical support. We also appreciate Dr. SungJun Back and Dr. DongRak Lee for their advice. This work is financially supported by the Ministry of Education and Human Resources Development (MOE), the Ministry of Commerce, Industry and Energy (MOCIE) and the Ministry of

Labor (MOLAB) through the fostering project of the Lab of Excellency. This research was also supported in part by the Institute of Advanced Machinery and Design at Seoul National University.

- H. Lee, K. Hong and E. Kim, 2004. Measurement protocol of women's nude breasts using a 3D scanning technique. *Applied Ergonomics* 35.
- H. Seo, F. Cordier and K. Hong, 2007. A breast modeler base on analysis of breast scans. *Computer Animation and Virtual Worlds* 2007.

REFERENCES

- W. Lee and N. Magnenat-Thalmann, 2000. Fast head modeling for animation. *Journal Image and Vision Computing*.
- M. Zhang, et al., 2004. Image-Based 3D Face Modeling. *Proceeding of the International Conference on CGIV'04*.
- R. Balaniuk, I. Costa and J. Melo, 2006. Cosmetic Breast Surgery Simulation. *VIII Symposium on Virtual Reality - SVR2006*.
- W. Lee, J. Gu and N. Magnenat-Thalmann, 2000. Generation Animatable 3D Virtual Humans from Photographs. *Computer Graphics Forum (Eurographics 2000)*.
- J.C. Gower and G.B. Dijksterhuis, 2004. *Procrustes Problems*, Oxford University Press.
- A.N. Ansari and M. Abdel-Mottaleb, 2003. 3-D Face Modeling Using Two Views and a Generic Face Model with Application to 3-D Face Recognition. In *Proceedings of the IEEE Conference on Advanced Video and Signal Based Surveillance*.
- U. Neumann, et al., 1999. Constructing a Realistic Head Animation Mesh for a Specific Person. *USR-TR*.
- J.C. Carr, et al., 1997. Surface interpolation with radial basis functions for medical imaging. *IEEE Transactions Medical Imaging*.
- D. Ruprecht and H. Müller, 1993. Free form deformation with scattered data interpolation methods. *Geometric Modelling (Computing Supplement 8)*, Springer Verlag., Wien.
- R.Y. Tsai, 1987. A Versatile Camera Calibration Technique for High-Accuracy 3D Machine Vision Metrology Using Off-the-Shelf TV Cameras and Lens. *IEEE Journal of Robotics and Automation*.
- A. Hilton, D. Beresford, T. Gentils, R. Smith and W. Sun, 1999. *Virtual People: Capturing Human Models to Populate Virtual Worlds*. Computer Animation, Geneva, Switzerland.
- T. Goto, W. Lee and N. Magnenat-Thalmann, 2002. Facial feature extraction for quick 3D face modeling. *Signal processing: Image communication*.
- W. Lee, P. Kalra and N. Magnenat-Thalmann, 1997. Model Based Face Reconstruction for Animation. In *Proc. Multimedia Modeling (MMM'97)*.
- J. Noh, D. Fidaleo and U. Neumann, 2000. Animated Deformations with Radial Basis Functions. *ACM Virtual Reality and Software Technology (VRST)*.
- J.C. Carr, et al., 2001. Reconstruction and Representation of 3D Objects with Radial Basis Functions. *Annual Conference Series*.
- I.K. Park, et al., 2005. Image-Based 3D Face Modeling System. *EURASIP Journal on applied signal processing*.